Generalized Correlation for Loading in Packed Towers with Countercurrent Gas-liquid Flow

J. E. HOWKINS and J. F. DAVIDSON

Cambridge University, Cambridge, England

Experiments in which a liquid film runs over a vertical string of spheres surrounded by a concentric tube through which air is blown upward have shown that loading in a packed tower is due to the formation of standing waves on the liquid film. In the ball-and-tube system a wave is formed just below the equator of each ball, owing to the pressure gradient within the air stream as it accelerates through the narrowing gap between the ball and the tube. Interfacial shear and surface tension are of secondary importance. The similarity between the characteristics of the ball-and-tube system and those of the randomly packed tower suggests that loading in the latter system is also due to wave formation. With this concept of loading, a correlation has been derived.

The importance of loading and flooding in the design of packed towers for countercurrent gas-liquid flow is well known, and numerous correlations for the prediction of these phenomena have been proposed (*1* to *4*), but none of them are based on a clear understanding of the detailed mechanism of loading and flooding. In a previous paper (*5*) the authors suggested that loading is due to the formation of standing waves on the liquid film within the packing. The present paper gives further support to this idea, which has been used as the basis for a correlation to predict the loading point with countercurrent gas-liquid flow.

The proposed mechanism involves a balance between the forces shown in Figure 1, which depicts an element of liquid running down the packing in a region where the gas is accelerating as it moves upward. The acceleration is due to contraction of the flow area available to the gas, and it follows from Bernoulli's theorem that there must be a pressure gradient within the gas stream and that consequently the pressure at P is greater than at Q, giving a net upward force on

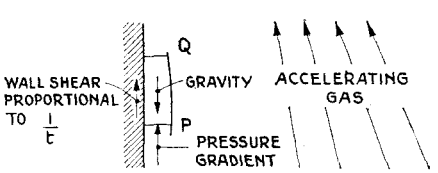

Fig. 1. Forces on an element of the liquid film of thickness t.

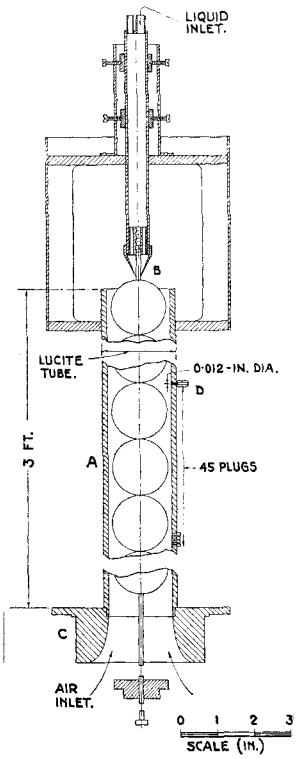

Fig. 2. Sectional scale drawing of the ball-and-tube apparatus.

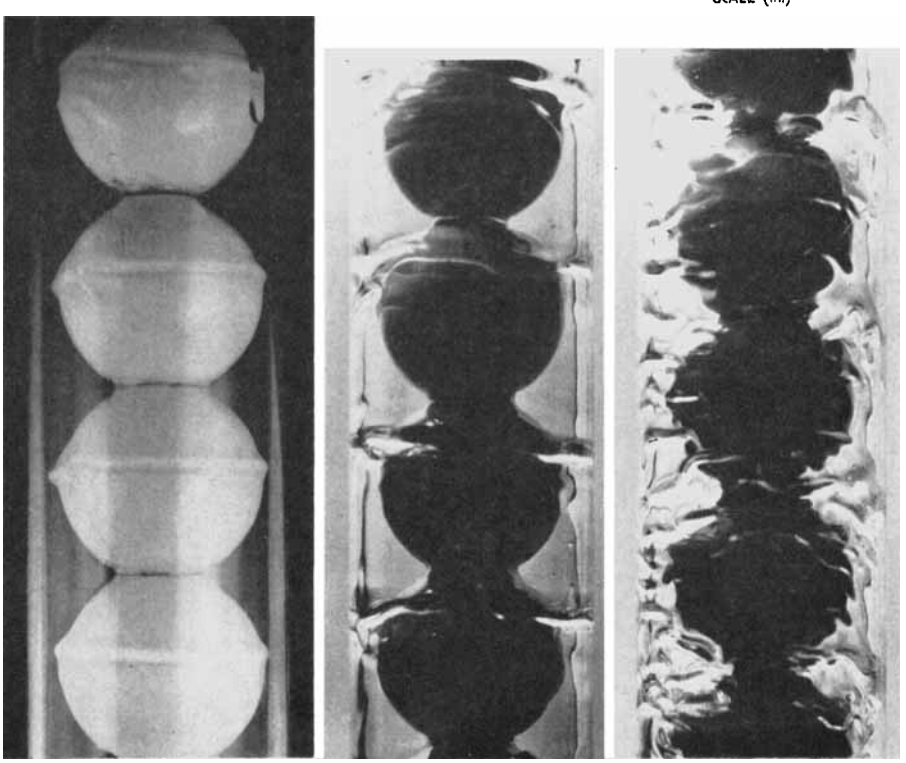

A *B* *C*

Fig. 3. Liquid paraffin ($\mu \simeq$ 300 centipoises) flowing over 1.49-in.-diameter balls inside 1.75-in.-diameter tube.

	(*A*) Loading	(*B*)	(*C*) Flooding
Liquid rate cc./min. =	6	6	6
Air rate cu. ft./min. =	4.31	4.87	6.06

J. E. Howkins is with Standard Oil Company, Sarnia, Ontario, Canada.

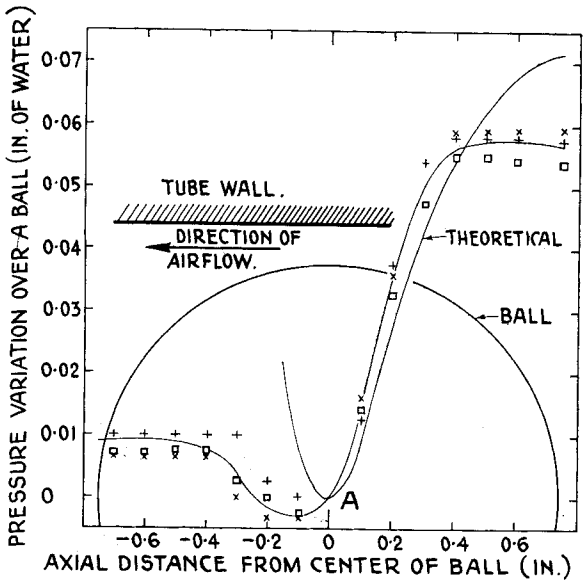

Fig. 4. The pressure distribution along the tube beside three successive balls: first, ⊡; second, ×; third, +.

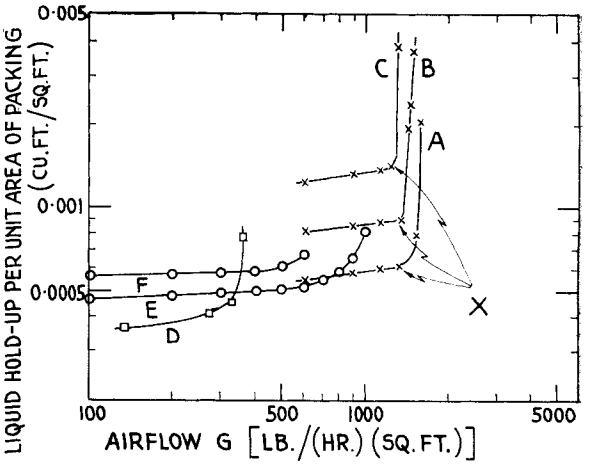

Fig. 6. Variation of holdup with air flow. *A*, *B*, *C*: 1.49-in. balls in 1.75-in. tube with water rates of 117, 860, and 3,410 lb./(hr.) (sq. ft.); *D* (*12*): 0.5-in. balls (random) in 2.89-in. column with water rate of 3,170 lb./(hr.)(sq. ft.); *E*, *F* (*13*): 0.5-in. rings in 10-in. column with water rates of 1,000 and 3,500 lb./(hr.)(sq. ft.)

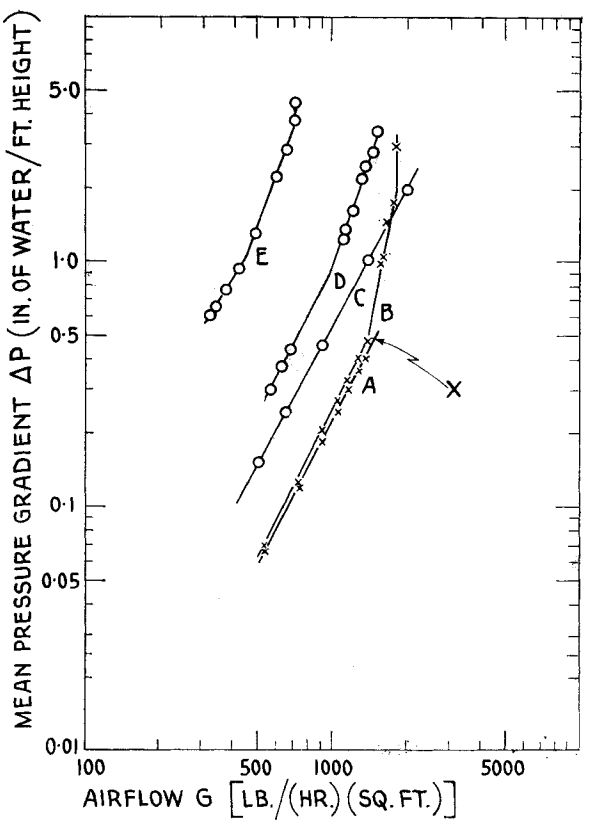

Fig. 5. Variation of mean pressure gradient with air flow. 1.49-in. balls in 1.75-in. tube: *A* = no liquid, *B* = water rate of 117 lb./(hr.)(sq. ft.); 8.66-in. column with 1-in. ceramic rings (*9*): *C* = no liquid, *D* = water rate of 1,250 lb./(hr.)(sq. ft.), *E* = water rate of 12,500 lb./(hr.)(sq. ft.).

the element of liquid. As the gravity force is balanced by the sum of the pressure gradient and wall shear forces and since the latter force is inversely proportional to the film thickness t, the accelerating gas flow must increase t. It can easily be seen that there must be a maximum gas flow beyond which the film cannot run down, because at a certain gas flow the pressure-gradient force will balance the gravity force and the film thickness must become very large if the viscous force is to be small. This kind of instability is thought to give an explanation of the phenomenon of loading and was investigated by the authors (*5*), using an apparatus specially designed for studying the instability rather than for simulating the behavior of packed towers.

This paper is a detailed study of what is thought to be a good, though simplified, model of a packed tower. The model consists of a vertical string of spheres covered by a liquid film and surrounded by a concentric tube through which gas is blown upward. At a certain gas flow a small wave is formed on the liquid film just below the equator of each sphere. The forces in Figure 1 account for the appearance of the waves, which form, as would be expected, near the point of maximum gas acceleration and pressure gradient. Measurements of pressure variation up the tube, together with theoretical calculations, make it clear that the wave formation is due to the pressure gradient balancing the gravity forces.

That the wave formation corresponds to loading in a packed tower is clear from a study of the holdup and pressure-drop characteristics and a comparison of them with the corresponding characteristics for packed towers. This comparison of characteristics shows that the ball-and-tube system is a good model of a packed

tower. The coincidence of the wave formation with the loading point for the ball-and-tube system, as determined from the pressure-drop and holdup characteristics, suggests strongly that loading in a packed tower is due to wave formation within the interstices. This being the case, the dimensionless groups used in the theory for predicting wave formation are applicable to the correlation of loading points. The resulting correlation is not entirely satisfactory in that it is semiempirical and for a given packing the loading points have to be determined experimentally at two liquid rates.

This concept of loading due to pressure-gradient forces rather than to interfacial shear accords with the calculations of Chilton and Colburn (*6, 7*), who showed that with single-phase flow in a packed tower the over-all pressure drop is due largely to repeated accelerations and that wall friction is of secondary importance.

APPARATUS AND PROCEDURE

The ball-and-tube apparatus, shown in Figure 2, was designed to fit into the air distributor and liquid separator described in the previous paper (*5*). A string of table-tennis balls of 1.49-in. diameter was held concentrically within a Lucite tube *A* of 1.75-in. bore. Water was fed onto the top ball through the annular gap between the end of the conical nozzle *B* and the ⅛-in.-diameter rod carrying the balls. Adjacent to the liquid inlet at the top of the apparatus was a small outlet tube, normally blanked off, which was used to eliminate air. The water ran uniformly in a thin film over the outside of the spheres and was removed at the bottom by the ⅛-in.-diameter rod which passed through the centers of the spheres. Air after being uniformly distributed passed through the Lucite orifice *C*, up the tube between the inner wall and the balls, and out to atmosphere at the top.

The pressure variation was measured over the whole column and across three balls in the middle of a string of twenty. This number was enough to counteract end effects, as shown by the similar pressure profiles across each of the three middle balls (Figure 4). The pressure tappings were formed by forty-six holes of equal diameter, drilled at 0.1-in. pitch in a straight line down the tube. Because of the sharp variations in pressure, the final tapping was 0.012 in. in diameter. The holes were normally plugged, but, when a measurement of the pressure was required, a plug was replaced by the tapping *D*, which was connected to a Chattock gauge measuring the pressure to ±1%. In Figure 2 the top tapping is ready for use and the forty-five holes below are plugged.

Balls and tubes of other diameters (without pressure tappings) were used to investigate the effect of size and voidage on the loading velocities. Orifice *C* was changed, but the general layout of the apparatus was the same as in Figure 2. Liquid paraffin was used in place of water to find the effect of higher viscosity.

Liquid holdup on the 1.49-in. balls was measured by recirculating the liquid and fixing all the volumes in the system except the volume of a graduated tank into which the liquid flowed from the column. Changes in level within the tank gave changes in holdup, and the total holdup was obtained by adding the initial holdup with zero airflow, obtained from data of Cullen (*8*), who used a weighing technique.

Behavior

The general behavior of the system is shown in Figure 3. Low air rates have a small effect on the liquid film and merely increase the amplitude of moving ripples, which are present at all but very low liquid rates. At a critical air rate the stationary waves shown in Figure 3*A* are formed, the initial formation being just below the equator of each ball. With water the wave breaks into spray as soon as it is formed; with liquid paraffin the wave is stable and is blown up above the equator, as in Figure 3*A*. At higher air rates the motion shown in Figures 3*B* and *C* is induced, the tube as well as the balls being covered with liquid. Ultimately flooding is reached, when liquid will not run out of the base of the apparatus.

RESULTS: LOADING DUE TO WAVE FORMATION

Pressure Variation over a Single Ball

Figure 4 shows the results from the forty-six tappings in the wall of the 1.75-in.-diameter tube, with 1.49-in. balls and no liquid flow. The results from the three successive balls have been made to agree at point *A*, and their similarity at other points shows that end effects are small. In the accelerating region the results agree, as would be expected, with simple theory based on Bernoulli's theorem, uniform flow across each horizontal section being assumed. Downstream there is a small pressure recovery, followed by a constant-pressure wake in the same way as with an infinite stream flowing past a sphere.

Over-all Pressure Drop

Figure 5 shows the mean pressure gradient as a function of air flow, both in the dry ball-and-tube system and with a constant liquid rate, and the results from randomly packed towers given by Sarchet (*9*) are also shown. The following points of similarity may be noted:

1. With no liquid flow, ln ΔP is a linear function of ln G, the slope being about 1.9 for the ball-and-tube system and for the randomly packed tower, where ΔP is the mean pressure gradient and G is the superficial gas rate.

2. With liquid flowing, the relation between ΔP and G is similar in both systems. The loading point is followed in each case by a line of increased slope. For the ball-and-tube system it is known from visual observation that the loading point X is coincident with the wave formation shown in Figure 3*A*; it therefore seems likely that loading in a randomly packed tower is due to wave formation in the converging parts of the packing.

Holdup

It has been found (*10, 11*) for packed towers that holdup is a function primarily of the liquid rate up to the loading point and that above the loading point the holdup increases sharply with gas flow. The ball-and-tube system behaves similarly, as shown in Figure 6, where holdup is plotted as a function of air flow at constant liquid rates. The point at which standing waves are formed is marked by an X. The increase in holdup after loading is sharper for the ball-and-tube system than for the randomly packed tower, as is consistent with the idea that loading is due to wave formation within the interstices. In the randomly packed tower, wave formation would be expected first in the most serious restrictions, and holdup would increase in these regions (in the manner of Figure 3*B*) before wave formation had begun in the other parts of the tower. The loading process would not be complete until wave formation had begun in all parts of the packing. With the ball-and-tube system, loading occurs all at once throughout the tower and the increase in holdup is therefore sharper.

THEORETICAL DEVELOPMENT OF THE GENERALIZED CORRELATION

The basic assumptions for the generalized correlation are as follows. (*See* Figure 7.)

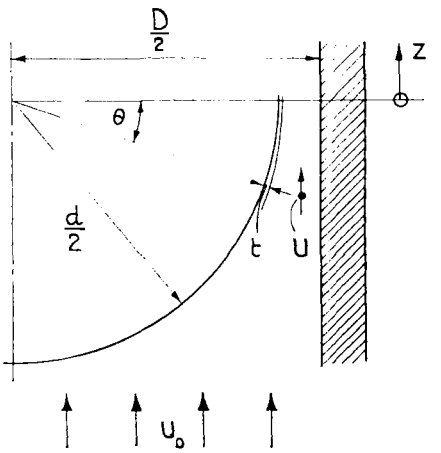

Fig. 7. Ball and tube with liquid film.

1. The viscosity of the air is neglected and its velocity across any horizontal section is assumed uniform. This assumption is justified by the agreement between theory and experiment in Figure 4. From continuity

$$U = \frac{U_0}{1 - \frac{d^2}{D^2}\cos^2\theta - \frac{4dt}{D^2}\cos^2\theta} \quad (1)$$

From Bernoulli's theorem

$$\frac{dp}{dz} = -\rho_G U \frac{dU}{dz} \qquad (2)$$

2. The liquid-film thickness is calculated from a balance between the forces in Figure 1. The velocity is assumed to be a parabolic function of distance measured normal to the surface, and since the surface of the ball is nearly vertical where the wave is formed, $\cos\theta \simeq 1$. The film thickness is therefore calculated by neglecting the kinetic energy of the liquid in the same way as in reference *5*:

$$t = \left[\frac{3\mu D^2 L}{4d\rho_L(\rho_L g + dp/dz)}\right]^{\frac{1}{3}} \qquad (3)$$

From Equation (3) it is clear that $-dp/dz$ cannot exceed $\rho_L g$, and in the previous paper (*5*) it was shown that wave formation occurs when

$$\frac{-dp}{dz} = \alpha\rho_L g \qquad (4)$$

where α is less than unity and varies from system to system. α can be predicted theoretically by relaxation methods (*5*), but in the present paper it will be left as an unknown parameter.

To give dp/dz at the wave crest, Equation (1) is differentiated, with the simplification that $dt/dz = 0$ at the wave crest. In Equation (1) it is also permissible to put $t\cos^2\theta \simeq t$ since the wave is formed near the equator, and using the resulting expression for dU/dz with Equations (2) and (4) gives the condition for loading:

$$\frac{4U_0^2 d\sin\theta}{D^2\left(1 - \frac{d^2}{D^2}\cos^2\theta - \frac{4dt}{D^2}\right)^3} = \frac{\alpha\rho_L g}{\rho_G} \qquad (5)$$

Table 1. Loading Correlation

[Equation (9)]

Reference		Ball and tube: Ball diam., in.	Ball and tube: Tube diam., in.	A	B	$\alpha = \frac{1.195A}{(1-\epsilon)^{1/2}(3\epsilon-1)^{5/2}}$
		1.49	1.75	0.032	26	0.51	0.27
		1.00	1.22	0.058	14	0.55	0.31
		0.50	0.63	0.064	5.9	0.58	0.25
		1.96	2.50	0.066	21	0.60	0.23
		1.49	2.00	0.11	21	0.64	0.26
		1.49	2.50	0.16	21	0.77	0.20
(*14*)	Quartz, 2 in. Serrated grids			0.015	63	0.46	0.27
(*14*)	2 in.			0.16	77	0.83	0.18
(*14*)	1.5 in. Stacked rings			0.10	41	0.89	0.10
(*14*)	3-in. stoneware Random rings			0.058	31	0.76	0.075
(*13*)	0.5-in. stoneware			0.024	16	0.61	0.075
(*14*)	1-in. carbon			0.018	23	0.66	0.039
(*13*)	1-in. carbon			0.032	22	0.70	0.055
(*13*)	1.5-in. stoneware			0.028	28	0.72	0.044
(*13*)	1.0-in. stoneware			0.032	25	0.73	0.048
(*14*)	1.0-in. stoneware			0.030	19	0.80	0.035
(*14*)	0.5-in. metal			0.024	13	0.87	0.024
(*14*)	2.0-in. metal			0.033	31	0.92	0.034

This equation can be generalized by writing d and D in terms of the voidage, ϵ, and a, the wetted area per unit volume:

$$\left.\begin{aligned}\epsilon &= 1 - \frac{2d^2}{3D^2}\\ a &= \frac{4d}{D^2}\end{aligned}\right\} \qquad (6)$$

The wave will be formed where $-dp/dz$ is maximum, and to find the angle where this occurs it is necessary to put $d^2p/dz^2 = 0$. Using Equations (1), (2), and (6), with $t = 0$ and $2z = -d\sin\theta$, gives the angle for maximum pressure gradient:

$$\sin^2\theta = \frac{3\epsilon - 1}{15(1-\epsilon)} \qquad (7)$$

This equation gives the angle for maximum pressure gradient in the absence of the liquid film and will therefore be applicable only at very low liquid rates. Eliminating t, dp/dz, θ, d, and D from Equations (3) to (7) gives the final condition for loading:

$$\frac{G^2 a}{\alpha\rho_G\rho_L g}\left[\frac{3\epsilon-1}{15(1-\epsilon)}\right]^{\frac{1}{3}}\left[\frac{5}{3(3\epsilon-1)}\right]^3 = 1 - \frac{5}{3\epsilon-1}\left[\frac{3La^2\mu}{(1-\alpha)\rho_L{}^2 g}\right]^{\frac{1}{3}} \qquad (8)$$

This may be written in the form

$$\frac{1}{A}\left(\frac{G^2 a}{\rho_G\rho_L g}\right) = 1 - B\left(\frac{La^2\mu}{\rho_L{}^2 g}\right)^{\frac{1}{3}} \qquad (9)$$

where A and B are functions which are given in terms of the packing dimensions by Equation (8) for the ball-and-tube system but have to be determined experimentally for other packings. The area a has not been included in the constants A and B to keep them dimensionless.

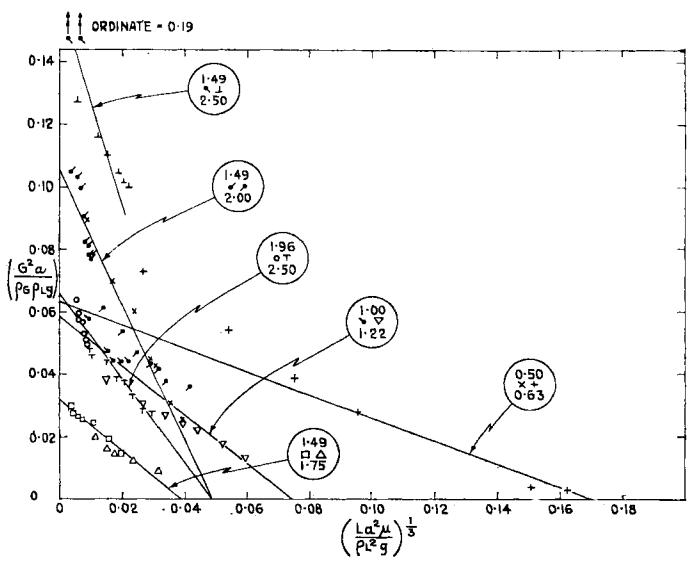

Fig. 8. Determination of A and B, Equation (9), for the ball-and-tube systems. In each circle the upper and lower numbers are the ball and tube diameters. The left-hand symbol is for air-water; the other is for air–liquid paraffin.

APPLICATION OF THE CORRELATION

To get A and B in Equation (9), $G^2a/\rho_G\rho_L g$ at loading is plotted as a

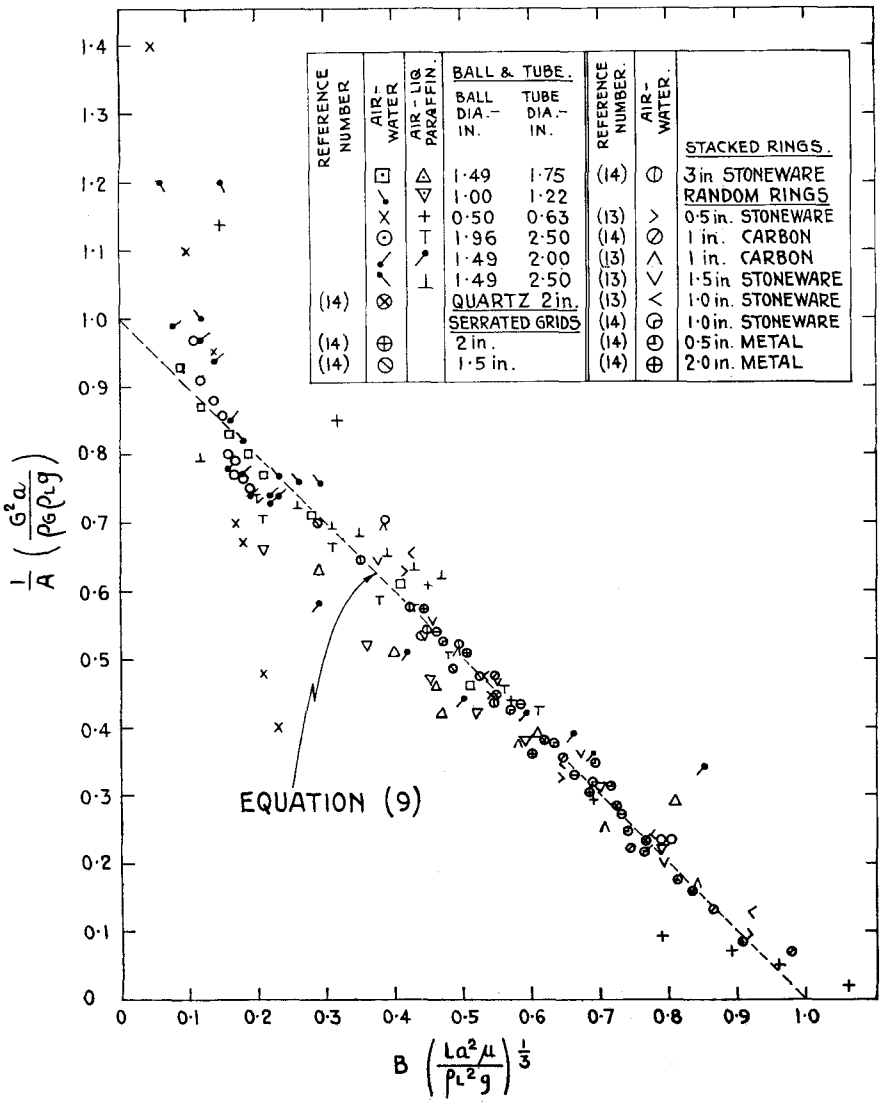

Fig. 9. Generalized loading correlation.

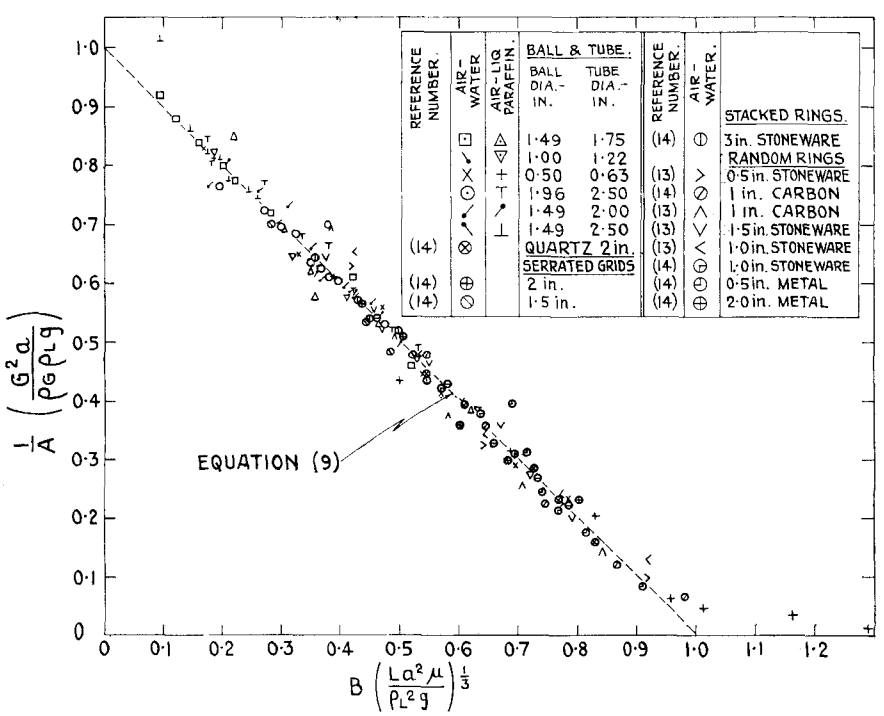

Fig. 10. Nongeneralized loading correlation.

function of $(La^2\mu/\rho_L^2 g)^{1/3}$ and A and B are determined from the best straight line through the points. Figure 8 shows the results for the ball-and-tube system, and similar graphs were plotted by means of the data for various packed towers of Shulman, Ullrich, and Wells (*13*) and Morris and Jackson (*14*). Table 1 shows the resulting values of A and B, which were used to replot all the results in Figure 9. The points from references *13* and *14* were selected from smoothed experimental data as the original data were not available. It is not certain whether the original data would give a better or worse scatter than is shown in Figure 9.

Validity of the Correlation

In Figure 8 the agreement between the results with water and liquid paraffin for the same system is satisfactory except in the case of the 0.50-in. balls, where the poor correlation is thought to be the effect of surface tension, which was not allowed for in the derivation of Equation (9) and is magnified with smaller packing.

The agreement between experiment and theory in Figure 9 indicates that the mechanism of loading in the ball-and-tube system is similar to the mechanism in the other packings.

A further check on the validity of the theory is given in Figure 10, which is similar to Figure 9, but with different values of A and B for each liquid. To get Figure 10, Figure 8 was redrawn, the behavior of each ball-and-tube system being represented by two straight lines, one for water and one for liquid paraffin. Essentially, Figure 10 is a plot of G^2 against $L^{1/3}$, since A, B, a, ρ_L, ρ_G, and μ are fixed for any one system, and it shows very good agreement with theory. The fact that Figure 10 is a better correlation than Figure 9 indicates that the constants A and B are not entirely independent of liquid viscosity for a particular system. This is further indicated in Figure 8, where for any ball-and-tube system the results are somewhat scattered around the fitted straight line; Figures 8 and 9, nevertheless, correlate the results reasonably well and justify the assumption that, to a first approximation, A and B are independent of liquid viscosity for each packing.

The theory can also be checked by calculating α, which is a measure of the maximum pressure gradient within the packing, in terms of liquid head. It should be somewhat less than unity, and its significance will be discussed later, with reference to interfacial shear. α can be calculated for the ball-and-tube system, because in this case Equations (8) and (9) should be identical. A and B can therefore be related to α and ϵ, and, the latter being known, two values of α are calculable, one from A and one from B. In the derivation of Equations (7) and (8), however, it was assumed that the

liquid-film thickness t was negligible. It would therefore be expected that the constant A, which depends upon the loading-gas rate at L and t being equal to zero, would give reasonable values of α. B, which gives a measure of the variation in the loading-gas rate due to finite liquid-film thicknesses, would not be expected to give a reasonable estimate of α. These assumptions are confirmed by calculation; Table 1 shows values of α calculated from the experimental values of A, but values of α calculated from B are nearly unity and in one case negative and have not been included.

Factors Affecting Loading

1. *Liquid Viscosity.* The viscosity of the liquid paraffin was about 300 times that of water, and the agreement obtained between the two sets of results for the ball-and-tube systems indicates that the final correlation, Equation (9), could be used for an approximate prediction of the behavior of randomly packed towers with any liquid when the air-water results are used. This method could not be applied to small packings.

2. *Interfacial Shear.* The approximate dependence of A and B on ϵ and the relative constancy of α (Table 1) indicate that the neglect of interfacial shear in deriving Equation (8) is justified. As was explained above, α may be thought of as the maximum pressure gradient within the packing in feet of liquid per foot of height and cannot exceed unity. In reference 5 α was about 0.6 and the difference from unity was attributed partly to interfacial shear and partly to interaction between the water film and the air stream. In Table 1, α is about 0.25 for the ball-and-tube system, and simple boundary-layer calculations showed that the lower value is due to interfacial shear.

Strictly, it is not possible to calculate α for the other packings, since its relation to A is not known. However, the values in Table 1, calculated from the ball-and-tube formula, indicate interesting trends. The serrated grids show, as might be expected, the greatest similarity to the ball-and-tube system. For the random packings it is not clear whether the low values of α are due to the packing geometry or to interfacial shear; however, the success of Equation (9) in correlating all the results indicates that shear is of secondary importance in randomly packed towers.

3. *Surface Tension.* In Figures 8 and 9, the results for the 0.50-in. balls are extremely scattered, probably because of surface tension, which would affect the loading point by stabilizing the wave and by altering the shape of the interstitial meniscus. Both these effects would be magnified for smaller packings and would be different for water and liquid paraffin, the surface tension of the latter being approximately 30 dynes/cm.

4. *Voidage* ϵ. The effect of increasing voidage is to move the point of wave formation. Table 2 shows the angle below the equator for maximum pressure gradient, calculated from Equation (7). It was difficult to observe the position of the initial waves on the balls, because as soon as the waves were formed they were pushed above the equator as in Figure 3*A*. At very high voidages, however, a wave formed on the lowest ball of the series at a point well below the equator, as would be expected from Table 2; a detailed treatment of this special case is given elsewhere (*15*). It is interesting to note that in the present experiments the 1.49-in. balls in the 2.50-in. tube loaded by wave formation on the bottom ball with air and water, and that therefore the resulting points on Figure 9 have a large deviation from Equation (9).

Table 2. Angle for Wave Formation

[Equation (7)]

ϵ	0.333	0.4	0.5	0.6	0.7	0.8
θ degrees	0	9	15	21	30	43

CONCLUSIONS

1. Loading in a packed tower is caused by the formation of standing waves on the liquid film at points within the packing where the pressure gradient, due to acceleration of the gas, is maximum. In a randomly packed tower loading is thought to be a gradual process, the wave formation occurring over a small range of air flows, although the evidence for this is not direct.

2. At large voidages loading will start at the bottom, and the practice of putting larger, and possibly graded, packing at the bottom is a good one.

3. Interfacial shear has a secondary effect on loading and is most important at large voidages.

4. Surface tension has a secondary effect on loading, although it is quite important for small sizes of packing.

5. Equation (9), which is a linear relation between the dimensionless velocity head in the gas and the dimensionless liquid-film thickness, is suitable for correlating loading points. The correlation is semiempirical, because constants A and B have to be determined for each packing by measuring the loading point at two liquid rates. The loading point at other liquid rates, and for different gases and liquids, can then be predicted.

ACKNOWLEDGMENT

J. E. Howkins wishes to acknowledge the support given by a Gas Council Scholarship to enable him to carry out this work.

NOTATION

A = packing constant
$$= \alpha\left[\frac{15(1-\epsilon)}{3\epsilon-1}\right]^{\frac{1}{2}}\left[\frac{3(3\epsilon-1)}{5}\right]^{3}$$
for the ball-and-tube system

a = interfacial area, sq. ft./cu. ft.

B = packing constant
$$= \frac{1}{(1-\alpha)^{\frac{1}{3}}}\left[\frac{5\times 3^{\frac{1}{3}}}{3\epsilon-1}\right]$$
for the ball-and-tube system

D = tube internal diameter, ft.

d = ball diameter, ft.

G = superficial gas rate, lb./(hr.)(sq. ft.)

g = acceleration of gravity

L = superficial liquid rate, lb./(hr.)(sq. ft.)

ΔP = mean pressure gradient, in. water/ft. height

p = pressure, lb./(ft.)(hr.^{2})

t = liquid-film thickness, ft.

U = gas velocity at any section, ft./hr.

U_0 = gas velocity in the empty tube, ft./hr.

z = axial distance, ft.

Greek Letters

α = fraction defined by Equation (4)

ϵ = voidage

θ = angle indicated in Figure 7

μ = liquid viscosity, lb./(ft.)(hr.)

ρ_G = gas density, lb./cu. ft.

ρ_L = liquid density, lb./cu. ft.

LITERATURE CITED

1. Sherwood, T. K., G. H. Shipley, and F. A. L. Holloway, *Ind. Eng. Chem.*, **30**, 765 (1938).
2. Bain, W. A., and O. A. Hougen, *Trans. Am. Inst. Chem. Engrs.*, **40**, 29 (1944).
3. Dell, F. R., and H. R. C. Pratt, *J. Appl. Chem. (London)*, **2**, 429 (1952).
4. Hoffing, E. H., and F. J. Lockhart, *Chem. Eng. Progr.*, **50**, 94 (1954).
5. Davidson, J. F., and J. E. Howkins, *Proc. Roy. Soc. (London)*, **240A**, 29 (1957).
6. Chilton, T. H., and A. P. Colburn, *Ind. Eng. Chem.*, **23**, 913 (1931).
7. ———, *Trans. Am. Inst. Chem. Engrs.*, **26**, 178 (1931).
8. Cullen, E. J., Ph.D. thesis, Univ. Cambridge, England (1956).
9. Sarchet, B. R., *Trans. Am. Inst. Chem. Engrs.*, **38**, 283 (1942).
10. Leva, Max, "Tower Packings and Packed Tower Design," p. 35, United States Stoneware Co., Akron, Ohio (1953).
11. Piret, E. L., C. A. Mann, and Thomas Wall, *Ind. Eng. Chem.*, **32**, 861 (1940).
12. Elgin, J. C., and F. B. Weiss, *Ind. Eng. Chem.*, **31**, 435 (1939).
13. Shulman, H. L., C. F. Ullrich and N. Wells, *A.I.Ch.E. Journal*, **1**, 247 (1955).
14. Morris, G. A., and J. Jackson, "Absorption Towers," pp. 24, 25, 38, 39, Butterworths, London, (1953).
15. Howkins, J. E., and J. F. Davidson, *Chem. Eng. Sci.*, **7**, 235 (1958).

Manuscript received Aug. 14, 1957; revised Jan. 20, 1958; accepted Feb. 6, 1958.